arXiv:1209.5463v1 [cond-mat.supr-con] 25 Sep 2012

Topological superfluid in a fermionic bilayer optical lattice

Ya-Jie Wu,[1] Jing He,[1] Chun-Li Zang,[1] and Su-Peng Kou[1,*]

[1] *Department of Physics, Beijing Normal University, Beijing 100875, China*

In this paper, a topological superfluid phase with Chern number $\mathcal{C} = \pm 1$, possessing gapless edge states and non-Abelian anyons is designed in a $\mathcal{C} = \pm 1$ topological insulator proximity to an s-wave superfluid on an optical lattice with the effective gauge field and layer-dependent Zeeman field coupled to ultracold fermionic atoms pseudo spin. We also study its topological properties and calculate the phase stiffness by using the random-phase-approximation approach. Finally we derive the temperature of the Kosterlitz-Thouless transition by means of renormalized group theory. Owning to the existence of non-Abelian anyons, this $\mathcal{C} = \pm 1$ topological superfluid may be a possible candidate for topological quantum computation.

I. INTRODUCTION

Topological quantum computation, based on the manipulation of non-Abelian anyons[1, 2], is considered as an effective method to deal with decoherence in realizing quantum computation. The first proposed candidate is the fractional quantum Hall state at filling factor $\nu = 5/2$ in ultra high-mobility samples [3, 4]. Other proposals are based on two dimensional (2D) chiral $p_x + ip_y$ superconductors with $\mathcal{C} = \pm 1$(the Chern-number) topological invariable[5] and then the s-wave-superconductor-topological-insulator systems[6, 7]. Among these approaches, accurate manipulations of single quasi-particles remains a major difficulty and new techniques are to be expected to overcome this drawback.

On the other hand, cold atoms in optical lattices are an extensively developing research field[8, 9]. Because one can precisely controls over the system parameters and defect-free properties, ultracold atoms in optical lattices provide an ideal platform to study many interesting physics in condensed matters[10, 11]. Some pioneering works revealed the promising potential of applying ultracold atoms to make quantum computer and quantum simulator. Recently, experimental realizations of quantum many-body systems in optical lattices have led to a chance to simulate strongly correlated electronic systems. By changing the intensity, phase and polarization of incident laser beams, one can tune the Hamiltonian parameters including the dimension, the hopping strength and the particle interaction at will.

In this paper, we propose a scenario in which a topological phase, possessing gapless edge states and non-Abelian anyons, is realized by proximity effect between a $\mathcal{C} = \pm 1$ topological insulator and an s-wave superfluid (SF) of ultracold fermionic atoms in an bilayer optical lattice with an effective gauge field and a layer-dependent Zeeman field generated by laser-field[12–18]. At the beginning, we give an effective design of the bilayer Haldane model. Then we put two-component (two pseudo-spins) interacting fermions on this bilayer optical lattice with fixed particle concentration. For layer-1, the Haldane model of two-component fermions at 1/4 filling under a strong Zeeman field becomes a $\mathcal{C} = \pm 1$ topological insulator. While for layer-2, there is no Zeeman fields, we get an s-wave SF state by tuning the interaction between fermion via Feshbach resonance technique. Thus due to the proximity effect, we get an effective $\mathcal{C} = \pm 1$ topological SF state, of which the π-flux obeys non-Aelian statistics and becomes a non-Aelian anyon. Thus, this $\mathcal{C} = \pm 1$ topological superfluid (TSF) may be a possible candidate for topological quantum computation.

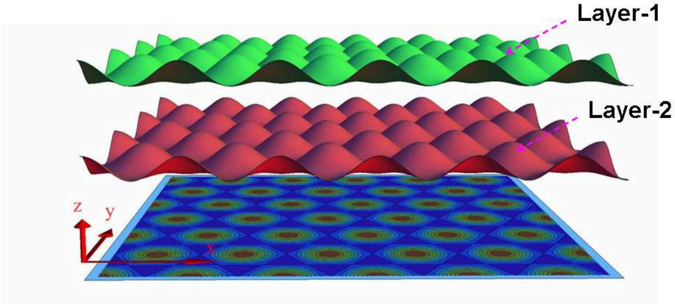

FIG. 1: The illustration of bilayer honeycomb optical lattice.

The paper is organized as follows. In Sec. II, we start with the Hamiltonian of the interacting spinful Haldane model on bilayer optical lattice. In Sec. III, we calculate the SF order parameter with mean field approach and get a global phase diagram at zero temperature. In Sec. IV, we point out that there exists a $\mathcal{C} = \pm 1$ TSF due to the proximity effect of the SF order in layer-2 on $\mathcal{C} = \pm 1$ topological insulator in layer-1. In Sec. V, we discuss the quantum properties of the $\mathcal{C} = \pm 1$ TSF, including the statistics of the π-flux and the edge states. In Sec. VI, by using random-phase-approximation (RPA), we calculate the phase stiffness of the $\mathcal{C} = \pm 1$ topological SF. In Sec.VII, we get the Kosterlitz-Thouless (KT) transition temperature by the renormalized group (RG) theory. Finally, the conclusions are given in Sec. VIII.

---

[*] Corresponding author; Electronic address: spkou@bnu.edu.cn

II. THE SPINFUL HALDANE MODEL ON A BILAYER OPTICAL LATTICE

In the first step, we design a bilayer optical lattice of the Haldane model. In Refs.[13], the monolayer optical lattice of the Haldane model had been proposed in the cold atoms with three blue detuned standing-wave lasers, of which the optical potential is given by

$$V(x,y)=\sum_{j=1,2,3} V_0\sin^2[k_L(x\cos\theta_j+y\sin\theta_j)+\pi/2] \quad (1)$$

where V_0 is the potential amplitude, $\theta_1=\pi/3$, $\theta_2=2\pi/3$, $\theta_3=0$, and k_L is the optical wave vector in XY plane[19]. On the other hand, to design a bilayer optical lattice, the optical potential from the interference of two opposite-traveling standing-wave laser beams along the z direction is added as

$$V(z)=V_L\sin^2(k_L^z z)-V_S\sin^2(2k_L^z z) \quad (2)$$

where V_L and V_S are the amplitudes of the long and short laser along the z-direction. k_L^z is the optical wave vector in z-direction. Thus the total optical potential of the bilayer honeycomb lattice in our case can be written as

$$V(x,y,z)=V(x,y)+V(z). \quad (3)$$

See the illustration in Fig.1. Since the potential barrier of the optical lattice along the z direction is a double well (See Fig.2), the vertical tunneling between different bilayer systems is suppressed seriously, each bilayer can be regarded as an independent 2D honeycomb lattice. The positions with a minimum potential along z-direction are $k_L^z z=2\pi n\pm\arccos\left[\sqrt{V_L/(4V_s)}\right]$ where n is an integer number.

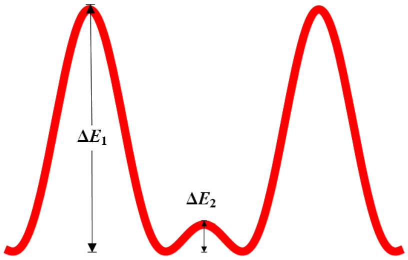

FIG. 2: The optical lattice potential along z-direction as a double well potential for $\Delta E_1\gg\Delta E_2$.

Let's calculate the tight-binding model of the bilayer optical lattice. Firstly we derive the hopping parameter $t_\perp$ between two layers. From Fig.2, for $0<V_L\leq 4V_S$ and $\Delta E_1=V_L+\frac{(4V_S-V_L)^2}{16V_S}\gg\Delta E_2=\frac{(4V_S-V_L)^2}{16V_S}$ or $(4V_S-V_L)\to 0$, one can see that the optical lattice potential along z-direction can be approximately reduced into a double well potential around $z=0$. Then we can expand $V(z)$ at $z=0$ and get

$$V(z)\simeq\frac{16V_S-V_L}{3}\left(k_L^z z\right)^4-\left(4V_S-V_L\right)\left(k_L^z z\right)^2. \quad (4)$$

We denote $|0\rangle_+$ and $|0\rangle_-$ as the two nearly degenerate ground states of the double well in the right-hand and left-hand wells, respectively. The corresponding eigenstates of the Hamiltonian are odd and even states $|0\rangle_e$ and $|0\rangle_o$ which are superposition of $|0\rangle_\pm$ such that $|0\rangle_o=1/\sqrt{2}\left(|0\rangle_+-|0\rangle_-\right)$, and $|0\rangle_e=1/\sqrt{2}\left(|0\rangle_++|0\rangle_-\right)$ with eigenvalues $E_0\pm\Delta E_0/2$, respectively. ΔE_0 is the splitting of the energy levels due to the quantum tunneling effect. We identify ΔE_0, i.e., the hopping parameter $t_\perp$.

According to the instanton approach[20, 21], we obtain the instanton solution as

$$z_{cl}\left(\tau\right)\equiv\pm\frac{1}{k_L^z}\sqrt{\frac{3\left(4V_S-V_L\right)}{2\left(16V_S-V_L\right)}}\tanh\left[\frac{\omega_\perp}{2}\left(\tau-\tau_0\right)\right] \quad (5)$$

and then get the energy level splitting ΔE_0 that corresponds to $t_\perp$ as[20, 21]

$$t_\perp=\Delta E_0/2=2\sqrt{\frac{3(S_c)_\perp}{2\pi}}\omega_\perp e^{-(S_c)_\perp} \quad (6)$$

where the trapping frequency $\omega_\perp$ is

$$\omega_\perp=\sqrt{\frac{\partial^2V(z)}{m\partial z^2}\mid_{z=z_{\min}}}=\sqrt{8\left(4V_S-V_L\right)E_r^z}, \quad (7)$$

with $z_{\min}$ being the value of z when $V(z)$ is a minimal value and the classical action $(S_c)_\perp$ of instanton is

$$(S_c)_\perp=\frac{\sqrt{2}\left(4V_S-V_L\right)}{\left(16V_S-V_L\right)}\sqrt{\frac{\left(4V_S-V_L\right)}{E_r^z}}. \quad (8)$$

$E_r^z=\frac{(k_L^z)^2}{2m}$ is the recoiling energy of the atoms in the z-direction where m is the mass of atoms. We have set $\hbar=1$.

Secondly we calculate the nearest neighbor hopping t. The optical lattice potential on XY plane is $V(x,y)$ as shown in Eq. (1) which forms a honeycomb lattice and simulate the Haldane Model. Substituting $\theta_1=\frac{\pi}{3}$, $\theta_2=\frac{2\pi}{3}$, $\theta_3=0$ in $V(x,y)$, we may get

$$V(x,y)=\frac{V_0}{2}\{3+\cos[\kappa(\frac{\sqrt{3}y+x}{2})]+\cos[\kappa(\frac{\sqrt{3}y-x}{2})]+\cos[\kappa x]\} \quad (9)$$

with $\kappa=2k_L$. Around the site A or B in Fig.3, we find $V(x,y)=3V_0^2\kappa^2(x^2+y^2)/16-3V_0/4$, i.e.,

$$V(x,y)=m\omega_0^2r^2/2-3V_0/4 \quad (10)$$

with $\omega_0=\sqrt{3V_0E_r^L}$, where $E_r^L=k_L^2/(2m)$. Here we may use the the Wentzel, Kramers and Brillouin (WKB) method that has been extended to two dimensions to estimate t for honeycomb lattice. From the Ref. [22], the semiclassical estimation of the tunneling amplitude reads

$$t=0.707(\frac{V_0}{E_r^L})^{3/4}e^{-0.685\sqrt{\frac{V_0}{E_r^L}}}E_r^L. \quad (11)$$

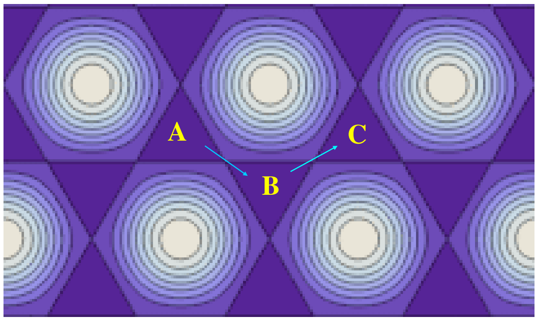

FIG. 3: The instanton process from A to C that leads to a next nearest neighbor hopping, t'.

Finally we calculate the next nearest neighbor hopping t'. The situation here is much different from that of t and $t_{\perp}$. The energy level splitting between two wells (denoted by A and C) shown in Fig.3 is due to the quantum tunneling process from A to B then to C. Now we obtain t' to be

$$t^{'} \simeq \sqrt{2}te^{-S_c} = (\frac{V_0}{E_r^L})^{3/4} e^{-1.370\sqrt{\frac{V_0}{E_r^L}}} E_r^L. \tag{12}$$

The coefficient 2 in e^{-2S_c} comes from twice of single instanton from one site to the nearest neighbor site. In this sense, we have

$$t^{'}/t \simeq \sqrt{2}e^{-S_c} = 1.414e^{-0.685\sqrt{V_0/E_r^L}} \tag{13}$$

which is always a small value. For example, if we set $V_0 = 23.806E_r^L$, the hopping parameters are given to be $t = 0.269E_r^L$ and $t' = 0.05t$.

Thus when two-component fermions are put into this bilayer honeycomb optical lattice, we may get an effective bilayer Haldane model by applying the Raman laser beams. Taking the tight-binding limit, we can superpose the Bloch states to obtain eight sets of Wannier functions $w_{A/B,\alpha,\sigma}(\mathbf{r} - \mathbf{r}_{A/B}) = \sqrt{\frac{1}{\pi l^2}} \exp[-r^2/(2l^2)]$, where $l = \sqrt{\hbar/(m\omega_0)}$ with $\omega_0 = \sqrt{3V_0E_r^L}/\hbar$, of which the recoil energy reads $E_r^L = \hbar^2k_L^2/(2m)$ and m is a single particle mass. Here A, B denote two-sublattice, $\alpha = 1$, 2 denote the index of the layer and $\sigma =\uparrow, \downarrow$ denote (pseudo-)spin degree of freedom, respectively. Then the two-component fermions in 2D bilayer honeycomb optical lattice has a Hamiltonian as[23]

$$\hat{H}_{\text{bi}} = -t \sum_{\langle i,j\rangle,\alpha,\sigma} \hat{c}_{i,\alpha,\sigma}^{\dagger}\hat{c}_{j,\alpha,\sigma} - t' \sum_{\langle\langle i,j\rangle\rangle,\alpha,\sigma} e^{\mathrm{i}\phi_{ij}} \hat{c}_{i,\alpha,\sigma}^{\dagger}\hat{c}_{j,\alpha,\sigma} \tag{14}$$
$$- t_{\perp} \sum_{i,\sigma} \hat{c}_{i,1,\sigma}^{\dagger}\hat{c}_{i,2,\sigma} + h.c.,$$

where $\hat{c}_{i,\alpha,\sigma}^{\dagger}$ ($\hat{c}_{i,\alpha,\sigma}$) represents fermion creation (annihilation) operators at site i of layer-α ($\alpha = 1$ or 2) for spin σ ($\uparrow$ or $\downarrow$). t (t') is the real nearest (next nearest) neighbor hopping amplitude, and $t_{\perp}$ is the interlayer coupling which is much smaller than t, i.e., $t_{\perp} \ll t$. $\langle i, j\rangle$, $\langle\langle i, j\rangle\rangle$ denote the nearest neighbor and the next nearest neighbor links, respectively. The next nearest neighbor hopping term has a complex phase $\phi_{ij} = \pm\frac{\pi}{2}$, where the positive phase is set clockwise. To design a complex phase of the next nearest neighbor hopping for a two-component fermions generated by the gauge field on the optical lattice, we may apply a Raman laser beams in XY plane with spacial-dependent Rabi frequencies as $\Omega_0 \sin(\tilde{k}_L x + \frac{\pi}{4})e^{\mathrm{i}y\tilde{k}}$ and $\Omega_0 \cos(\tilde{k}_L x + \frac{\pi}{4})e^{-\mathrm{i}y\tilde{k}}$ ($\tilde{k}_L = \frac{2\pi}{3a}$) where a denotes the length between nearest neighbour lattice sites. Then we get a laser-field-generated effective gauge field on this honeycomb optical lattice similar to that proposed for the monolayer honeycomb optical lattice in Ref.[13].

In addition, we apply a layer-dependent Zeeman field to polarize spin degree of freedom by detuning Raman lasers only on the fermions in layer-1 as

$$\hat{H}_{\text{Zeeman}} = h \sum_{i,\sigma,\sigma'} \hat{c}_{i,1,\sigma}^{\dagger}\sigma_{\sigma,\sigma'}^{z}\hat{c}_{i,1,\sigma'}. \tag{15}$$

For big enough Zeeman field h, this term eventually drives this fermion model at 1/4 filling in layer-1 to a $\mathcal{C} = \pm 1$ topological insulator with fixed chemical potential $\mu_1 = -h$. Such layer-dependent Zeeman field can be realized by the a modulated laser wave along z-direction, of which the wave vector is k_L^z but has an additional phase shift to the laser beams that generate the optical lattice, $\Delta\phi = 2\pi - \arccos\left[\sqrt{V_L/(4V_s)}\right]$. For this case, we always get a zero Zeeman field at layer-2 at positions with a minimum potential along z-direction $k_L^z z = 2\pi n - \arccos\left[\sqrt{V_L/(4V_s)}\right]$ but a finite Zeeman field at layer-1 at positions with a minimum potential along z-direction $k_L^z z = 2\pi n + \arccos\left[\sqrt{V_L/(4V_s)}\right]$.

Furthermore, we consider a strong interaction via Feshbach resonance technique[24, 25] and contact interaction

$$\hat{H}_U = -U \sum_{i,\alpha=1,2} \hat{n}_{i,\alpha,\uparrow}\hat{n}_{i,\alpha,\downarrow} \tag{16}$$

where $U > 0$ is the on-site attractive interaction strength given by integrals over the Wannier function around site A or B that reads

$$U = -g\int d\mathbf{r} \left|w(\mathbf{r} - \mathbf{r}_{A/B})\right|^4 \tag{17}$$
$$\simeq 2\sqrt{3}\{[\ln(k_L^2b^2/4)]^{-1} + \Delta\mathcal{B}/(\mathcal{B} - \mathcal{B}_0)\}\sqrt{V_0E_r^L}$$

where g is coupling constant in two dimension[26], b is radius of hard-sphere potential, $\mathcal{B}$ is magnetic field, $\mathcal{B}_0$ is resonance magnetic field and $\Delta\mathcal{B}$ is the width of the resonance, respectively.

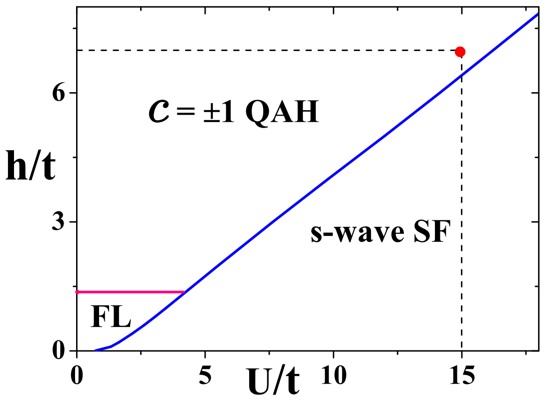

FIG. 4: The phase diagram of fermions (filling factor $n_f = 1/4$) with attractive interaction on layer-1 honeycomb optical lattice for the case of $t' = 0.05t$. There exist three quantum phases: $\mathcal{C} = \pm1$ QAH state, s-wave SF state and Fermi liquid state (FL). In this paper we only consider the $\mathcal{C} = \pm1$ QAH state of $h = 7t$ which is marked by the red dot.

Finally we get an interacting two-component fermions system in 2D bilayer honeycomb optical lattice of the Haldane model with layer-dependent Zeeman field as[23, 27, 28]

$$\hat H = \hat H_{\mathrm{bi}} + \hat H_{\mathrm{Zeeman}} + \hat H_U + \hat H_c. \tag{18}$$

where

$$\hat H_c = -\mu_1 \sum_{i,\sigma} \hat c^\dagger_{i,1,\sigma}\hat c_{i,1,\sigma} - \mu_2 \sum_{i,\sigma} \hat c^\dagger_{i,2,\sigma}\hat c_{i,2,\sigma} \tag{19}$$

with μ_1 and μ_2 denoting the chemical potentials in layer-1 and layer-2, respectively.

III. MEAN FIELD APPROACH AND GLOBAL PHASE DIAGRAM

Considering a tiny interlayer coupling $t_\perp$, we may use the mean field approach separately for each layer. When increasing the interaction strength, the fermionic system described in Eq.(18) is unstable against superfluid (SF) orders that are described by $\triangle_{1,2}$ for s-wave pairing order parameters as $\Delta_1 = \langle \hat c_{i,1,\downarrow}\hat c_{i,1,\uparrow}\rangle$ and $\Delta_2 = \langle \hat c_{i,2,\downarrow}\hat c_{i,2,\uparrow}\rangle$. Due to the layer-dependent Zeeman field, the symmetry between two layers is broken ($\Delta_1 \neq \Delta_2$). In this section, we give the mean field calculations. Due to tiny interlayer coupling, we may do calculations of the models for each layer separately.

Firstly, we consider the interacting Haldane model on layer-1 as

$$\begin{aligned}\hat H_1 = {} & -t \sum_{\langle i,j\rangle,\sigma} \hat c^\dagger_{i,1,\sigma}\hat c_{j,1,\sigma} - t' \sum_{\langle\langle i,j\rangle\rangle,\sigma} e^{\mathrm{i}\phi_{ij}} \hat c^\dagger_{i,1,\sigma}\hat c_{j,1,\sigma} \qquad (20)\\ & - \mu \sum_{i,\sigma} \hat c^\dagger_{i,1,\sigma}\hat c_{i,1,\sigma} + h \sum_{i,\sigma,\sigma'} \hat c^\dagger_{i,1,\sigma}\sigma^z_{\sigma,\sigma'}\hat c_{i,1,\sigma'} \\ & - U \sum_i \hat n_{i,1,\uparrow}\hat n_{i,1,\downarrow} + h.c..\end{aligned}$$

When there are a finite s-wave pairing order parameters of layer-1 $\Delta_1 = \langle \hat c_{i,1,\uparrow}\hat c_{i,1,\downarrow}\rangle$, we get the effective Hamiltonian as

$$\begin{aligned}\hat H_{1,\mathrm{eff}} = {} & -t \sum_{\langle i,j\rangle,\sigma} \hat c^\dagger_{i,1,\sigma}\hat c_{j,1,\sigma} - t' \sum_{\langle\langle i,j\rangle\rangle,\sigma} e^{\mathrm{i}\phi_{ij}} \hat c^\dagger_{i,1,\sigma}\hat c_{j,1,\sigma} \qquad (21)\\ & + h \sum_{i,\sigma,\sigma'} \hat c^\dagger_{i,1,\sigma}\sigma^z_{\sigma,\sigma'}\hat c_{i,1,\sigma'} - U \sum_i \Delta_1 \hat c_{i,1,\downarrow}\hat c_{i,1,\uparrow} \\ & - \mu \sum_{i,\sigma} \hat c^\dagger_{i,1,\sigma}\hat c_{i,1,\sigma} + h.c..\end{aligned}$$

The energy spectrums of the fermions in layer-1 are given by

$$\begin{aligned} (E_{1,k})_1 &= h + e_{1,k}, \quad (E_{1,k})_2 = h - e_{1,k} \\ (E_{1,k})_3 &= h + e_{2,k}, \quad (E_{1,k})_4 = h - e_{2,k} \end{aligned} \tag{22}$$

where

$$\begin{aligned} e_{1,k} &= \sqrt{\mu^2 + (U\Delta)^2 + \gamma_k^2 + |\xi_k|^2 + 2f}, \\ e_{2,k} &= \sqrt{\mu^2 + (U\Delta)^2 + \gamma_k^2 + |\xi_k|^2 - 2f}. \end{aligned} \tag{23}$$

The functions $|\xi_k|$, γ_k, f are

$$\begin{aligned} |\xi_k| &= t\sqrt{3 + 2\cos(\sqrt{3}k_y) + 4\cos(3k_x/2)\cos(\sqrt{3}k_y/2)}, \\ \gamma_k &= -t'[4\cos(3k_x/2)\sin(\sqrt{3}k_y/2) - 2\sin\sqrt{3}k_y], \\ f &= 2\sqrt{\gamma_k^2[\mu^2 + (U\Delta)^2] + |\xi_k|^2\mu^2}. \end{aligned} \tag{24}$$

By minimizing the ground state energy we arrive at the following self-consistent equations

$$\begin{aligned} \frac{1}{U} = \frac{1}{4N}\Big[& -\sum_{(E_{1,k})_1<0} \frac{1+\gamma_k^2/f}{e_{1,k}} \tanh\!\Big(-\frac{(E_{1,k})_1}{2T}\Big) \qquad (25)\\ & + \sum_{(E_{1,k})_2<0} \frac{1+\gamma_k^2/f}{e_{1,k}} \tanh\!\Big(-\frac{(E_{1,k})_2}{2T}\Big) \\ & - \sum_{(E_{1,k})_3<0} \frac{1-\gamma_k^2/f}{e_{2,k}} \tanh\!\Big(-\frac{(E_{1,k})_3}{2T}\Big) \\ & + \sum_{(E_{1,k})_4<0} \frac{1-\gamma_k^2/f}{e_{2,k}} \tanh\!\Big(-\frac{(E_{1,k})_4}{2T}\Big)\Big], \end{aligned}$$

and

$$n = 1 + \frac{\mu}{2N}[-\sum_{(E_{1,k})_1<0} \frac{1+(\gamma_k^2+|\xi_k|^2)/f}{e_{1,k}} \tanh(-\frac{(E_{1,k})_1}{2T}) \tag{26}$$

$$+ \sum_{(E_{1,k})_2<0} \frac{1+(\gamma_k^2+|\xi_k|^2)/f}{e_{1,k}} \tanh(-\frac{(E_{1,k})_2}{2T})$$

$$- \sum_{(E_{1,k})_3<0} \frac{1-(\gamma_k^2+|\xi_k|^2)/f}{e_{2,k}} \tanh(-\frac{(E_{1,k})_3}{2T})$$

$$+ \sum_{(E_{1,k})_4<0} \frac{1-(\gamma_k^2+|\xi_k|^2)/f}{e_{2,k}} \tanh(-\frac{(E_{1,k})_4}{2T})],$$

where n is fermion density and N is the number of primitive cells. By this approach we obtain the phase diagram given in Fig. 4.

Next we consider the interacting Haldane model on layer-2 as

$$\hat{H}_2 = -t \sum_{\langle i,j\rangle,\sigma} \hat{c}^\dagger_{i,2,\sigma}\hat{c}_{j,2,\sigma} - t' \sum_{\langle\langle i,j\rangle\rangle,\sigma} e^{i\phi_{ij}} \hat{c}^\dagger_{i,2,\sigma}\hat{c}_{j,2,\sigma}$$
$$- \mu \sum_{i,\sigma} \hat{c}^\dagger_{i,2,\sigma}\hat{c}_{i,2,\sigma} - U \sum_i \hat{n}_{2,i\uparrow}\hat{n}_{2,i\downarrow}. \tag{27}$$

of which the chemical potential is set to be equal to that of layer-1. Considering a finite s-wave pairing order parameters of layer-2 $\Delta_2 = \langle \hat{c}_{i,2,\uparrow}\hat{c}_{i,2,\downarrow}\rangle$, we get the effective Hamiltonian as

$$\hat{H}_{2,\mathrm{eff}} = -t \sum_{\langle i,j\rangle,\sigma} \hat{c}^\dagger_{i,2,\sigma}\hat{c}_{j,2,\sigma} - t' \sum_{\langle\langle i,j\rangle\rangle,\sigma} e^{\mathrm{i}\phi_{ij}} \hat{c}^\dagger_{i,2,\sigma}\hat{c}_{j,2,\sigma}$$
$$- U \sum_i \Delta_2 \hat{c}_{i,2,\downarrow}\hat{c}_{i,2,\uparrow} - \mu \sum_{i,\sigma} \hat{c}^\dagger_{i,2,\sigma}\hat{c}_{i,2,\sigma} + h.c.. \tag{28}$$

The energy spectrums of the fermions in layer-1 are given by

$$(E_{2,k})_1 = (E_{2,k})_2 = e_{1,k}, (E_{2,k})_3 = (E_{2,k})_4 = e_{2,k}.$$

Similarly, we get self-consistent equations as

$$\frac{1}{U} = \frac{1}{4N}[\sum_k \frac{1+\gamma_k^2/f}{e_{1,k}} \tanh(\frac{e_{1,k}}{2T}) \tag{29}$$
$$+ \sum_k \frac{1-\gamma_k^2/f}{e_{2,k}} \tanh(\frac{e_{2,k}}{2T})]$$

and

$$n = 1 + \frac{\mu}{2N}[\sum_k \frac{1+(\gamma_k^2+|\xi_k|^2)/f}{e_{1,k}} \tanh(\frac{e_{1,k}}{2T}) \tag{30}$$
$$\sum_k \frac{1-(\gamma_k^2+|\xi_k|^2)/f}{e_{2,k}} \tanh(\frac{e_{2,k}}{2T})].$$

By this approach we obtain the SF pairing order parameter given in Fig.5.

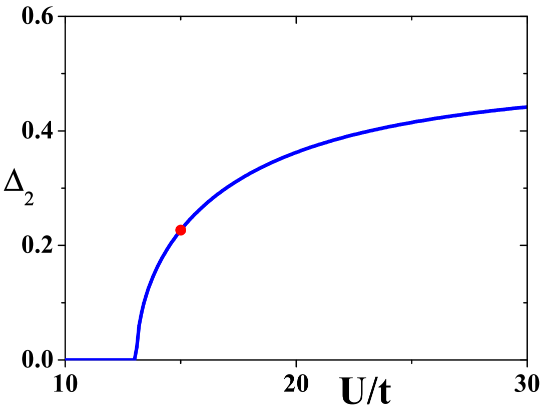

FIG. 5: SF order parameter of the fermion with attractive interaction on layer-2 honeycomb optical lattice for the case of $t' = 0.05t$. There exist two quantum phases: s-wave SF state and metal state. In this paper we only consider the s-wave SF state of $\mu_2 = -7t$ which is marked by the red point.

Now the total effective Hamiltonian is given by

$$\hat{H}_{\mathrm{eff}} = \hat{H}_{\mathrm{bi}} + \hat{H}_{\mathrm{Zeeman}} + \hat{H}_{SF} + \hat{H}_c, \tag{31}$$

where

$$\hat{H}_{SF} = -U \sum_{i,\alpha} \Delta_\alpha (\hat{c}_{i,\alpha,\downarrow}\hat{c}_{i,\alpha,\uparrow} + \hat{c}^\dagger_{i,\alpha,\uparrow}\hat{c}^\dagger_{i,\alpha,\downarrow}). \tag{32}$$

Thus we get four self-consistent equations of the fermions in both layers for $\Delta_{1,2}$ and $\mu_{1,2}$ by minimizing the ground state energy. We fix the fermion filling factor $n_f = 1/4$ in layer-1. A key point here is to keep the following chemical potential condition:

$$\mu_1 = \mu_2 \tag{33}$$

which guarantees 1/4 filling factor for the fermions in layer-1. To keep the above condition, we must tune the chemical potential μ_2 in layer-2 by manipulating the interaction U to synchronize with μ_1 in layer-1.

From Fig.4, one can see that for $U \neq 0$, there exist three quantum phases in layer-1: the Fermi liquid (FL), the topological insulator of $\mathcal{C} = \pm 1$ TKNN number with quantized anomalous Hall (QAH) effect (we also call it $\mathcal{C} = \pm 1$ QAH state) and s-wave superfluid (SF)[29]. For free fermions, $U = 0$, there exists a critical point for Zeeman field: $h_c \simeq 1.37t$. For the case of large Zeeman field, $h > h_c$, the ground state is $\mathcal{C} = \pm 1$ topological insulator with chiral edge states; For the case of smaller Zeeman field, $h < h_c$, the ground state is a FL state. When considering the interaction term, there may exist s-wave SF state, and the quantum phase transition from $\mathcal{C} = \pm 1$ QAH state to SF state is the first order. In this paper we consider the $\mathcal{C} = \pm 1$ QAH state with $h = 7t$. For this case, due to big imbalanced Fermi gaps of different spin components, the attracting interaction is irrelevant. The ground state is $\mathcal{C}=\pm 1$ QAH state until the interaction strength is larger than $16.3t$.

For layer-2, the situation is much different due to zero Zeeman field. Fig.5 shows the SF pairing order parameter Δ_2 of layer-2 for the case of $t'=0.05t$, $\mu_2=-7t$. For the weak interaction case, the ground state is FL; for the large interaction case, when $U>13.0t$, the ground state becomes SF with trivial topological properties. Just for this reason, we cannot get a $\mathcal{C}=\pm 1$ topological SF in a monolayer system, and thus have to turn to a bilayer system.

Now, we consider the model with the parameters $U=15t$, $h=7t$, $t'=0.05t$ (marked by the red spots in Fig.4 and Fig.5, respectively), at which we derived $\Delta_1=0$, $\Delta_2=0.227$, $\mu_1=\mu_2=-h=-7t$ at zero temperature. Thus we have a $\mathcal{C}=\pm 1$ QAH in layer-1 and an s-wave SF state in layer-2. Now the total Hamiltonian is given by

$$\begin{aligned}\hat{H}_{\text{eff}} = & -t\sum_{\langle i,j\rangle,\alpha,\sigma}\hat{c}^{\dagger}_{i,\alpha,\sigma}\hat{c}_{j,\alpha,\sigma}-t'\sum_{\langle\langle i,j\rangle\rangle,\alpha,\sigma}e^{\mathrm{i}\phi_{ij}}\hat{c}^{\dagger}_{i,\alpha,\sigma}\hat{c}_{j,\alpha,\sigma} \\ & -t_{\perp}\sum_{i,\sigma}(\hat{c}^{\dagger}_{i,1,\sigma}\hat{c}_{i,2,\sigma}+h.c.)+h\sum_{i,\sigma,\sigma'}\hat{c}^{\dagger}_{i,1,\sigma}\sigma^{z}_{\sigma,\sigma'}\hat{c}_{i,1,\sigma'} \\ & +h\sum_{i,\sigma}\hat{c}^{\dagger}_{i,1,\sigma}\hat{c}_{i,1,\sigma}+h\sum_{i,\sigma}\hat{c}^{\dagger}_{i,2,\sigma}\hat{c}_{i,2,\sigma} \\ & -U\sum_{i}\Delta_2(\hat{c}_{i,2,\downarrow}\hat{c}_{i,2,\uparrow}+\hat{c}^{\dagger}_{i,2,\uparrow}\hat{c}^{\dagger}_{i,2,\downarrow}).\end{aligned} \tag{34}$$

At high temperature, the SF pairing order disappears. The transition temperature of SF order in layer-2 is $k_BT_c\simeq 2.25t$.

IV. $\mathcal{C}=\pm 1$ TOPOLOGICAL SF DUE TO PROXIMITY EFFECT OF SF ORDER IN LAYER-2 ON $\mathcal{C}=\pm 1$ QAH IN LAYER-1

We use the purterbative theory to calculate the proximity effect of the SF order in layer-2 on the $\mathcal{C}=\pm 1$ QAH in layer-1. See the illustration in Fig.6. The Hamiltonian has a form as

$$\hat{H}_{\text{eff}}=\hat{H}_0+\hat{H}_I \tag{35}$$

in which

$$\begin{aligned}\hat{H}_0 = & -t\sum_{\langle i,j\rangle,\alpha,\sigma}\hat{c}^{\dagger}_{i,\alpha,\sigma}\hat{c}_{j,\alpha,\sigma}-t'\sum_{\langle\langle i,j\rangle\rangle,\alpha,\sigma}e^{\mathrm{i}\phi_{ij}}\hat{c}^{\dagger}_{i,\alpha,\sigma}\hat{c}_{j,\alpha,\sigma} \\ & +h\sum_{i,\sigma,\sigma'}\hat{c}^{\dagger}_{i,1,\sigma}\sigma^{z}_{\sigma,\sigma'}\hat{c}_{i,1,\sigma'}-\mu\sum_{i,\sigma}\hat{c}^{\dagger}_{i,1,\sigma}\hat{c}_{i,1,\sigma} \\ & -U\sum_{i}\Delta_{2,i}(\hat{c}_{i,2,\downarrow}\hat{c}_{i,2,\uparrow}+\hat{c}^{\dagger}_{i,2,\uparrow}\hat{c}^{\dagger}_{i,2,\downarrow})+h.c. \\ & -\mu\sum_{i,\sigma}\hat{c}^{\dagger}_{i,2,\sigma}\hat{c}_{i,2,\sigma}\end{aligned} \tag{36}$$

is the unperturbation term, and due to $t_{\perp}\ll U\Delta_2$ and the interlayer coupling

$$\hat{H}_I=-t_{\perp}\sum_{i,\sigma}\left(\hat{c}^{\dagger}_{i,1,\sigma}\hat{c}_{i,2,\sigma}+h.c.\right) \tag{37}$$

is the small perturbation term.

In the purterbative theory, we firstly use the path-integral representation

$$Z=\int[dc^{*}_{1,\sigma}dc_{1,\sigma}][dc^{*}_{2,\sigma}dc_{2,\sigma}]e^{-S_0-S'} \tag{38}$$

by replacing electronic operators $\hat{c}^{\dagger}_{i,\sigma}$ and $\hat{c}_{j,\sigma}$ to Grassmann variables $c^{*}_{i,\sigma}$ and $c_{j,\sigma}$. S_0 is the action as

$$S_0=\int d\tau\mathcal{L}_0 \tag{39}$$

and the Lagrangian in terms of Grassmann variables $c^{*}_{i,\sigma}$ and $c_{i,\sigma}$ is then obtained as

$$\mathcal{L}_0=\sum_{i,\alpha,\sigma}c^{*}_{i,\alpha,\sigma}\partial_{\tau}c_{i,\alpha,\sigma}+H_0(c^{*},c),$$

where $H_0(c^{*},c)$ is obtained by replacing operators in $\hat{H}_0$ with Grassman variables. S' is the action as

$$S'=\int d\tau\mathcal{L}' \tag{40}$$

where

$$\mathcal{L}'=-t_{\perp}\sum_{i,\sigma}\left(c^{*}_{i,1,\sigma}c_{i,2,\sigma}+h.c.\right). \tag{41}$$

Now we integrate $c^{*}_{2,i,\sigma}$ $c_{2,i,\sigma}$ and get

$$Z=\int[dc^{*}_{1,\sigma}dc_{1,\sigma}]e^{-(S_1)_0-S'_{\text{eff}}} \tag{42}$$

where

$$\begin{aligned}(S_1)_0 = \int d\tau[& \sum_{i,\sigma}c^{*}_{i,1,\sigma}\partial_{\tau}c_{i,1,\sigma}-t\sum_{\langle ij\rangle,\sigma}c^{*}_{i,1,\sigma}c_{j,1,\sigma} \\ & -\mu_1\sum_{i,\sigma}c^{*}_{i,1,\sigma}c_{i,1,\sigma}-t'\sum_{\langle\langle i,j\rangle\rangle,\sigma}e^{\mathrm{i}\phi_{ij}}c^{*}_{i,1,\sigma}c_{j,1,\sigma} \\ & +h\sum_{i,\sigma}c^{*}_{i,1,\sigma}\sigma^{z}c_{i,1,\sigma}+h.c.]\end{aligned} \tag{43}$$

and

$$S'_{\text{eff}}=-\ln\left\langle e^{-S'}\right\rangle_2 \tag{44}$$

where $\left\langle e^{-S'}\right\rangle_2=\int[dc^{*}_2dc_2]e^{-(S_2)_0-S'}$. Thus we have

$$\begin{aligned}\left\langle e^{-S'}\right\rangle_2 & = \int[dc^{*}_{2,\sigma}dc_{2,\sigma}]e^{-(S_2)_0-S'} \\ & \simeq e^{\left[\left\langle -S'\right\rangle_2+\frac{1}{2}\left(\left\langle S'^2\right\rangle_2-\left\langle -S'\right\rangle_2^2\right)+\cdots\right]}.\end{aligned} \tag{45}$$

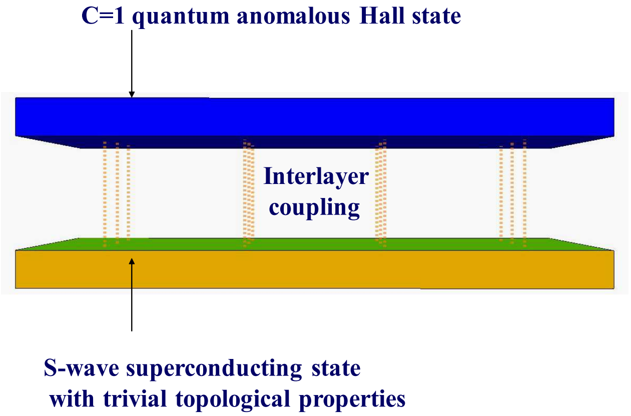
C=1 quantum anomalous Hall state
Interlayer coupling
S-wave superconducting state with trivial topological properties

FIG. 6: The illustration of $\mathcal{C} = \pm 1$ topological SF due to proximity effect between SF order in layer-2 and $\mathcal{C} = \pm 1$ QAH in layer-1.

Due to $\langle S' \rangle_2 = 0$ we derive

$$\begin{aligned} S'_{\rm eff} &= -\ln\left\langle e^{-S'}\right\rangle_2 \simeq -\frac{1}{2}\left\langle (S')^2\right\rangle_2 \\ &= \int d\tau[\sum_i \Delta_{1,\rm induce} c_{i,1,\downarrow} c_{i,1,\uparrow} + h.c.] \end{aligned} \tag{46}$$

where

$$\Delta_{1,\rm induce} = -\frac{(t_\perp)^2}{U\Delta_{i,2}}. \tag{47}$$

To derive this result we have used the following equation,

$$\begin{aligned} \left\langle (S')^2\right\rangle_2 &= \left\langle (t_\perp \sum_{i,\sigma} c^*_{i,1,\sigma} c_{i,2,\sigma} + h.c.)^2 \right\rangle_2 \\ &= 2t_\perp^2 \sum_i [c_{i,1,\downarrow} c_{i,1,\uparrow} \left\langle c^*_{i,2,\uparrow} c^*_{i,2,\downarrow}\right\rangle_2 \\ &+ c^*_{i,1,\uparrow} c^*_{i,1,\downarrow} \left\langle c_{i,2,\downarrow} c_{i,2,\uparrow}\right\rangle_2] \\ &= \frac{2t_\perp^2}{U\Delta_{2,i}} \sum_i \left[c_{i,1,\downarrow} c_{i,1,\uparrow} + c^*_{i,1,\uparrow} c^*_{i,1,\downarrow}\right] \end{aligned} \tag{48}$$

where

$$\left\langle c_{i,2,\downarrow} c_{i,2,\uparrow}\right\rangle_2 = \left\langle c^*_{i,2,\uparrow} c^*_{i,2,\downarrow}\right\rangle_2 = \frac{1}{U\Delta_{i,2}}. \tag{49}$$

That means although there is no SF pairing order parameter of fermions in layer-1, the tiny interlayer hopping will lead to an induced SF order due to the proximity effect. After integrating gapped fermions on layer-2, the low energy effective model of such bilayer system is finally reduced into

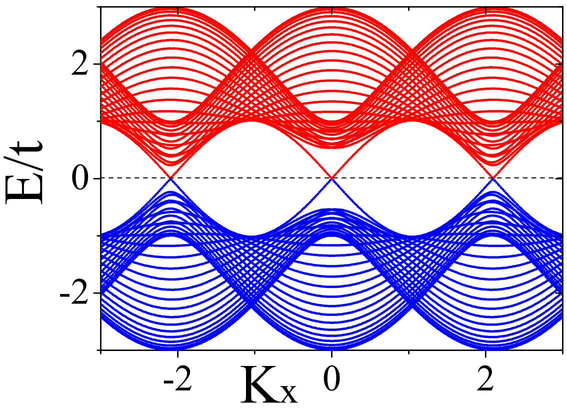

FIG. 7: The armchair edge state of $\mathcal{C} = \pm 1$ QAH with induced SF order on layer-1 and related parameters $U = 15t$, $h = 7t$, $\mu_1 = -7t$, $t' = 0.05t$, $\Delta_{1,\rm induce} = 0.001$.

$$\begin{aligned} \hat{H}_{1,\rm eff} &= -t \sum_{\langle i,j\rangle,\sigma} \hat{c}^\dagger_{i,1,\sigma} \hat{c}_{j,1,\sigma} - t' \sum_{\langle\langle i,j\rangle\rangle,\sigma} e^{\mathrm{i}\phi_{ij}} \hat{c}^\dagger_{i,1,\sigma} \hat{c}_{j,1,\sigma} \\ &+ h \sum_{i,\sigma,\sigma'} \hat{c}^\dagger_{i,1,\sigma} \sigma^z_{\sigma,\sigma'} \hat{c}_{i,1,\sigma'} + h \sum_{i,\sigma} \hat{c}^\dagger_{i,1,\sigma} \hat{c}_{i,1,\sigma} \\ &+ \sum_i \Delta_{1,\rm induce} \hat{c}_{i,1,\downarrow} \hat{c}_{i,1,\uparrow} + h.c. \end{aligned} \tag{50}$$

where $\Delta_{1,\rm induce}$ is the induced SF order parameter of fermions in layer-1 which is estimated by the perturbation approach as $\Delta_{1,\rm induce} \simeq -\frac{(t_\perp)^2}{U\Delta_2}$. And for a tiny induced SF order parameter, we always get a really large energy gap of the fermions in the bulk, $\Delta E \simeq 0.52t$, which protects the topological properties of the $\mathcal{C} = \pm 1$ topological SF order.

Thus due to the proximity effect between $\mathcal{C} = \pm 1$ QAH and s-wave SF, the ground state is really a $\mathcal{C} = \pm 1$ topological SF as

$$\mathcal{C} = \pm 1 \text{ QAH} + \text{s-wave SF} \rightarrow \mathcal{C} = \pm 1 \text{ TSF} \tag{51}$$

of which the topological properties is similar to that of 2D chiral $p_x + ip_y$ wave SF[30, 31].

V. TOPOLOGICAL PROPERTIES

In this section we will study its topological properties by calculating the edge states and the zero modes on a π-flux (vortex with half quantized "magnetic" flux).

In Fig.7, we show the gapless Majorana edge modes of this effective model on a lattice with open boundary condition along y-direction (armchair edge) and periodic boundary condition along x-direction.

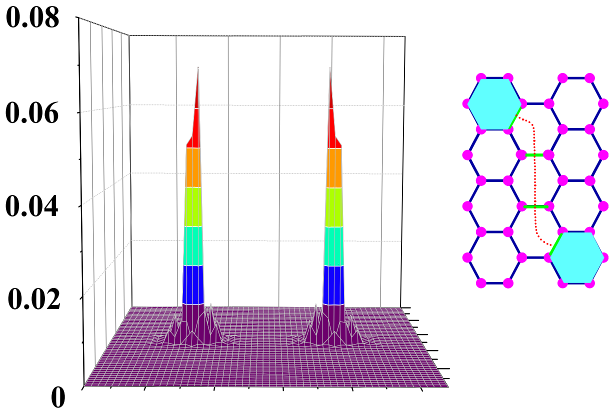

FIG. 8: The particle density of the zero modes of a pair of π-flux in $\mathcal{C}=\pm1$ QAH with induced SF order parameter on a 36×36 lattice in layer-1. In the right figure, there is a branch-cut (red dashed line) between two π-fluxes (cyan plaquette) which changes the signs of the hopping terms on green links.

In Fig.8 we demonstrate the existence of a single zero-mode on a π-flux obtained as a solution of the Bogoliubov-de Gennes equations [32, 33]. This is the Majorana zero energy mode and can be described by a real fermion field $\gamma^{\dagger}=\int dr[u_0\psi^{\dagger}+v_0\psi]$ $(\gamma^{\dagger}=\gamma)$[32]. When two π-fluxes are fused together (taken to the same plaquette in the honeycomb optical lattice), the result contains more than one quasiparticle due to the Ising fusion rule [34],

$$\sigma\times\sigma=I+\psi. \tag{52}$$

These results imply that the π-flux is a non-Abelian anyon (people also call it Ising anyon) obeying non-Abelian statistics as that in chiral $p_x+\mathrm{i}p_y$ wave SF. The topological properties of the $\mathcal{C}=\pm1$ topological SF order are similar to those of chiral $p_x+\mathrm{i}p_y$ superconductors with $\mathcal{C}=\pm1$ topological invariable.

VI. PHASE STIFFNESS OF $\mathcal{C}=\pm1$ TOPOLOGICAL SF ORDER

In this section, by using the random-phase-approximation, we calculate the phase stiffness of $\mathcal{C}=\pm1$ topological SF order which is determined by the phase fluctuations in layer-2. The Hamiltonian of fermions in layer-2 is

$$\hat{H}_{2,\mathrm{eff}}=-t\sum_{\langle i,j\rangle,\sigma}\hat{c}^{\dagger}_{i,2,\sigma}\hat{c}_{j,2,\sigma}-t'\sum_{\langle\langle i,j\rangle\rangle,\sigma}e^{\mathrm{i}\phi_{ij}}\hat{c}^{\dagger}_{i,2,\sigma}\hat{c}_{j,2,\sigma}-\mu\sum_{i,\sigma}\hat{c}^{\dagger}_{i,2,\sigma}\hat{c}_{i,2,\sigma}-U\sum_{i}\hat{n}_{i,2,\uparrow}\hat{n}_{i,2,\downarrow}+h.c.. \tag{53}$$

Thus in path-integral representation the partition function is given by

$$Z=\int[dc^{*}_{2,\sigma}dc_{2,\sigma}]e^{-S_2} \tag{54}$$

by replacing electronic operators $\hat{c}^{\dagger}_{i,2,\sigma}$ and $\hat{c}_{j,2,\sigma}$ to Grassmann variables $c^{*}_{i,2,\sigma}$ and $c_{j,2,\sigma}$. The effective action S_2 is

$$S_2=\int d\tau\mathcal{L}_2 \tag{55}$$

and the Lagrangian in terms of Grassmann variables is then obtained as

$$\mathcal{L}_2=\sum_{i,\sigma}c^{*}_{i,2,\sigma}\partial_{\tau}c_{i,2,\sigma}+H_{2,\mathrm{eff}}(c^{*}_{2,\sigma},c_{2,\sigma}), \tag{56}$$

where $H_{2,\mathrm{eff}}(c^{*}_{2,\sigma},c_{2,\sigma})$ is obtained by replacing the operators in $\hat{H}_{2,\mathrm{eff}}$ with Grassman variables.

Considering the s-wave pairing order parameter of layer-2 $\Delta_2=\langle\hat{c}_{2,i,\uparrow}\hat{c}_{2,i,\downarrow}\rangle$, we get the partition function as

$$Z=\int[dc^{*}_{2,\sigma}dc_{2,\sigma}][d\Delta^{*}d\Delta]e^{-S}, \tag{57}$$

where the action of fermions in layer-2 is

$$\begin{aligned}S=&\sum_{\omega_m,\mathbf{k}}(\mathrm{i}\omega_m+\gamma_{\mathbf{k}}-\mu)c^{*}_{\mathbf{k},\sigma}c_{\mathbf{k},\sigma}+2\beta\mu N\\&+\sum_{\omega_m,\mathbf{k}}\xi_{\mathbf{k}}c^{*}_{A,\mathbf{k},\sigma}c_{B,\mathbf{k},\sigma}+c.c.\\&-\frac{1}{\sqrt{N}}\sum_{k,q}(U\Delta^{*}(-q)c_{-\mathbf{k}+\mathbf{q}/\mathbf{2},\uparrow}c_{\mathbf{k}+\mathbf{q}/\mathbf{2},\downarrow}\\&+U\Delta(q)c^{*}_{\mathbf{k}+\mathbf{q}/\mathbf{2},\downarrow}c^{*}_{-\mathbf{k}+\mathbf{q}/\mathbf{2},\uparrow})+2\beta N\sum_{q}U\Delta^{*}(q)\Delta(q)\end{aligned} \tag{58}$$

with $\omega_m=(2n+1)\pi/\beta$ and $\omega_l=2n\pi/\beta$. We denote $k=(\mathrm{i}\omega_m,-\mathbf{k})$ and $q=(\mathrm{i}\omega_l,-\mathbf{q})$. After integrating over the fermionic field, the action turns into

$$S=2\beta N\sum_{q}U\Delta^{*}(\mathbf{q})\Delta(\mathbf{q})+2\beta\mu N-\sum_{k,k',q}\mathbf{Tr}\ln(G^{-1}), \tag{59}$$

where

$$G^{-1} = \begin{pmatrix} (\mathrm{i}\omega_m + \gamma_{\mathbf{k}} - \mu)\delta_{\mathbf{k},\mathbf{k}'} & -U\Delta(q) & \xi_k\delta_{\mathbf{k},\mathbf{k}'} & 0 \\ -U\Delta^*(-q) & (\mathrm{i}\omega_m + \gamma_{\mathbf{k}} + \mu)\delta_{\mathbf{k},\mathbf{k}'} & 0 & -\xi_k\delta_{\mathbf{k},\mathbf{k}'} \\ \xi_k^*\delta_{\mathbf{k},\mathbf{k}'} & 0 & (\mathrm{i}\omega_m - \gamma_{\mathbf{k}} - \mu)\delta_{\mathbf{k},\mathbf{k}'} & -U\Delta(q) \\ 0 & -\xi_k^*\delta_{\mathbf{k},\mathbf{k}'} & -U\Delta^*(-q) & (\mathrm{i}\omega_m - \gamma_{\mathbf{k}} + \mu)\delta_{\mathbf{k},\mathbf{k}'} \end{pmatrix}.$$

Then we consider the phase fluctuations on the SF order parameter and define $U\Delta(q) = \Delta_0 + \Lambda(q)$ where the mean field value Δ_0 is a real constant and $\Lambda(\mathbf{q})$ is complex fluctuating field. Thus G^{-1} is divided into two parts, i.e.,

$$G^{-1} = G_0^{-1} + G_1^{-1} \tag{60}$$

where

$$G_0^{-1} = \begin{pmatrix} \mathrm{i}\omega_m + \gamma_{\mathbf{k}} - \mu & -\Delta_0 & \xi_k & 0 \\ -\Delta_0 & \mathrm{i}\omega_m + \gamma_{\mathbf{k}} + \mu & 0 & -\xi_k \\ \xi_k^* & 0 & \mathrm{i}\omega_m - \gamma_{\mathbf{k}} - \mu & -\Delta_0 \\ 0 & -\xi_k^* & -\Delta_0 & \mathrm{i}\omega_m - \gamma_{\mathbf{k}} + \mu) \end{pmatrix}$$

and

$$G_1^{-1} = \begin{pmatrix} 0 & -\Lambda_A(q) & 0 & 0 \\ -\Lambda_A^*(-q) & 0 & 0 & 0 \\ 0 & 0 & 0 & -\Lambda_B(q) \\ 0 & 0 & -\Lambda_B^*(-q) & 0 \end{pmatrix}. \tag{61}$$

Using the expansion of the logarithm, one gets

$$\begin{aligned} \mathbf{Tr}\ln G^{-1} &= \mathbf{Tr}\ln(G_0^{-1} + G_1^{-1}) \qquad (62) \\ &= \mathbf{Tr}\ln G_0^{-1} - \frac{1}{2}\mathbf{Tr}(G_0 G_1^{-1} G_0 G_1^{-1}) \end{aligned}$$

Next we investigate the Gaussian fluctuations of the paring field $\Lambda(q)$ around the saddle point Δ_0[35, 36]. The fluctuation field is written as

$$\Lambda^\dagger(q) = (\Lambda_A^*(-q), \Lambda_A(q), \Lambda_B(q), \Lambda_B^*(-q)). \tag{63}$$

Then quadratic effective action becomes

$$S = S_0 + S_1 + 2\beta N \sum_q U\Delta^*(\mathbf{q})\Delta(\mathbf{q}) + 2\beta\mu N, \tag{64}$$

where

$$S_0 = \frac{\beta}{N}\mathbf{Tr}\ln G_0^{-1}, \tag{65}$$

$$S_1 = \frac{\beta}{2N}\sum_{\mathbf{q},\mathbf{k}} \Lambda^\dagger(\mathbf{q})Q(\mathbf{q},\mathbf{k})\Lambda(\mathbf{q}), \tag{66}$$

and the detailed form of elements in $Q(\mathbf{q},\mathbf{k})$ are shown in Appendix A. Using the Matsubara summation formula, one can obtain the quantities $Q_{i,j}$ above. Then in the static limit, i.e., $\mathrm{i}\omega_l \to 0$, at zero temperature, $Q_{i,j}$ can be described as follows, for example, if

$$Q_{i,j} = \sum_{\omega_m} G_{0bc}(k)G_{0gh}(k-q) \tag{67}$$

and then after the summation, it becomes

$$\begin{aligned} Q_{ij} = &-\frac{A_{bc}(\mathbf{k})B_{gh}(\mathbf{k}-\mathbf{q}) + B_{bc}(\mathbf{k})A_{gh}(\mathbf{k}-\mathbf{q})}{e_{1,\mathbf{k}-\mathbf{q}} + e_{1,\mathbf{k}}} \qquad (68) \\ &- \frac{A_{bc}(\mathbf{k})D_{gh}(\mathbf{k}-\mathbf{q}) + B_{bc}(\mathbf{k})C_{gh}(\mathbf{k}-\mathbf{q})}{e_{2,\mathbf{k}-\mathbf{q}} + e_{1,\mathbf{k}}} \\ &- \frac{C_{bc}(\mathbf{k})B_{gh}(\mathbf{k}-\mathbf{q}) + D_{bc}(\mathbf{k})A_{gh}(\mathbf{k}-\mathbf{q})}{e_{1,\mathbf{k}-\mathbf{q}} + e_{2,\mathbf{k}}} \\ &- \frac{C_{bc}(\mathbf{k})D_{gh}(\mathbf{k}-\mathbf{q}) + D_{bc}(\mathbf{k})C_{gh}(\mathbf{k}-\mathbf{q})}{e_{2,\mathbf{k}-\mathbf{q}} + e_{2,\mathbf{k}}}, \end{aligned}$$

where the parameters A_{ij}, B_{ij}, C_{ij}, D_{ij} are all shown in Appendix A.

In order to obtain the superfluid phase stiffness, we further separate the fluctuation into its amplitude and phase components $\Lambda_{A/B}(\mathbf{q}) = [\lambda_{A/B}(\mathbf{q}) + \mathrm{i}\theta_{A/B}(\mathbf{q})]/\sqrt{2}$ with real filed $\lambda_{A/B}(\mathbf{q})$ and $\theta_{A/B}(\mathbf{q})$. The changes of basis can be written as

$$\begin{pmatrix} \Lambda_A^*(-\mathbf{q}) \\ \Lambda_A(\mathbf{q}) \\ \Lambda_B(\mathbf{q}) \\ \Lambda_B^*(-\mathbf{q}) \end{pmatrix} = \frac{1}{\sqrt{2}} \begin{pmatrix} 1 & \mathrm{i} & 0 & 0 \\ 1 & -\mathrm{i} & 0 & 0 \\ 0 & 0 & -\mathrm{i} & 1 \\ 0 & 0 & \mathrm{i} & 1 \end{pmatrix} \begin{pmatrix} \lambda_A(\mathbf{q}) \\ \theta_A(\mathbf{q}) \\ \theta_B(\mathbf{q}) \\ \lambda_B(\mathbf{q}) \end{pmatrix}. \tag{69}$$

Then we have

$$S_1{=}\frac{\beta}{2}\sum_{\mathbf{q}}\lambda^*\left(\mathbf{q}\right)W\lambda(\mathbf{q}), \tag{70}$$

where $\lambda = \left(\begin{array}{cccc} \lambda_A(\mathbf{q}) & \theta_A(\mathbf{q}) & \theta_B(\mathbf{q}) & \lambda_B(\mathbf{q}) \end{array}\right)^T$, and the detailed forms of elements in matrix W are shown in Appendix A. Integrating over the gapped field $\lambda(\mathbf{q})$, in the static limit at zero temperature, we obtain

$$S_1[\theta] = \frac{\beta}{2}\sum_{\mathbf{q}}[\theta_A(\mathbf{q}), \theta_B(\mathbf{q})]X\begin{bmatrix}\theta_A(\mathbf{q})\\ \theta_B(\mathbf{q})\end{bmatrix} \tag{71}$$

with

$$X = \left(\begin{array}{cc} W_{22}-W_{B11} & W_{23}-W_{B12}\\ W_{32}-W_{B21} & W_{33}-W_{B22}\end{array}\right), \tag{72}$$

where the elements W_{B11}, W_{B12}, W_{B21}, W_{B22} become

$$\begin{aligned} W_{B11} &= W_{A11}W_{21}W_{12} + W_{A12}W_{21}W_{42} \\ &\quad + W_{A21}W_{24}W_{12} + W_{A22}W_{24}W_{42} \\ W_{B12} &= W_{A11}W_{21}W_{13} + W_{A12}W_{21}W_{43} \\ &\quad + W_{A21}W_{24}W_{13} + W_{A22}W_{24}W_{43} \\ W_{B21} &= W_{A11}W_{31}W_{12} + W_{A12}W_{31}W_{42} \\ &\quad + W_{A21}W_{34}W_{12} + W_{A22}W_{34}W_{42} \\ W_{B22} &= W_{A11}W_{31}W_{13} + W_{A12}W_{31}W_{43} \\ &\quad + W_{A21}W_{34}W_{13} + W_{A22}W_{34}W_{43} \end{aligned} \tag{73}$$

and the elements W_{A11}, W_{A12}, W_{A21}, W_{A22} are given by

$$\begin{aligned} W_{A11} &= \frac{W_{44}}{W_{11}W_{44}-W_{14}W_{14}} \\ W_{A12} &= \frac{-W_{14}}{W_{11}W_{44}-W_{14}W_{14}} \\ W_{A21} &= \frac{-W_{41}}{W_{11}W_{44}-W_{14}W_{14}} \\ W_{A22} &= \frac{W_{11}}{W_{11}W_{44}-W_{14}W_{14}}. \end{aligned} \tag{74}$$

At last, we arrive at the the effective action for phase fluctuations as

$$S[\theta] = \frac{\beta}{2}\sum_{\mathbf{q}}[\theta_A(\mathbf{q}), \theta_B(\mathbf{q})]T\begin{bmatrix}\theta_A(\mathbf{q})\\ \theta_B(\mathbf{q})\end{bmatrix} \tag{75}$$

where the elements of matrix T read

$$\begin{aligned} T_{11}(\mathbf{q}) &= \frac{1}{U} + (W_{22}-W_{B11}) \\ T_{12}(\mathbf{q}) &= (W_{23}-W_{B12}) \\ T_{21}(\mathbf{q}) &= (W_{32}-W_{B21}) \\ T_{22}(\mathbf{q}) &= \frac{1}{U} + (W_{33}-W_{B22}). \end{aligned} \tag{76}$$

We may derive the zero temperature superfluid stiffness $\rho_s(0)$ numerically in the static limit by identifying[35–37]

$$\sqrt{T_{11}(\mathbf{q})T_{22}(\mathbf{q})} - \sqrt{T_{12}(\mathbf{q})T_{21}(\mathbf{q})} = \frac{\sqrt{3}\rho_s(0)}{2}\mathbf{q}^2 \tag{77}$$

for $\mathbf{q}^2 \to 0$.

After obtaining the phase stiffness of $\mathcal{C} = \pm 1$ topological SF order, the effective Lagrangian of the phase fluctuations is obtained as

$$L_p = \frac{1}{2}\rho_s(0)(\nabla\theta)^2. \tag{78}$$

For example, for the case of $U = 15t$, $t' = 0.05t$, $\mu_1 = \mu_2 = -h = -7t$, we have a small phase stiffness as

$$\rho_s(0) \simeq 0.00286t.$$

VII. KOSTERLITZ-THOULESS TRANSITION

From above calculations, one can see that the induced SF pairing in layer-1 will be determined by the SF pairing in layer-2 as $\Delta_{1,\text{induce}} = -\frac{(t_\perp)^2}{U\Delta_2}$. If there exists a vortex in layer-2, $\Delta_{2,i} \to \Delta_2 \exp[\mathrm{i}\sum_{l\neq i}\operatorname{Im}\ln(z_i - z_l)]$, there will appear induced vortex in layer-1, $\Delta_{1,\text{induce},i} \to \Delta_{1,\text{induce}}\exp[-\mathrm{i}\sum_{l\neq i}\operatorname{Im}\,\ln(z_i - z_l)]$ where z_i is the position as $z_i = x_i + iy_i$. So we can only study the dynamics of vortices in layer-1 which is defined as

$$\theta_i = \sum_{l\neq i}\operatorname{Im}\ln(z_i - z_l) \tag{79}$$

where z_i is the vortex position as $z_i = x_i + iy_i$.

According to the above analysis, we can get the Kosterlitz-Thouless (KT) transition temperature by the renormalized group (RG) theory. For two vortices in layer-1, there exists a confinement potential as

$$V \simeq q^2 \ln\frac{|\mathbf{r}|}{a} \tag{80}$$

at $|\mathbf{r}| > a$, where $q^2 = 2\pi\rho_s(0)$, and $\mathbf{r}$ is the distance between the vortex and anti-vortex. With the increase of temperature, the vortex-antivortex pairs can be thermally excited, leading to a contribution to the screening effect by reducing V to $V_{\text{eff}} = \frac{1}{\kappa}V$, where κ denotes the dielectric constant. In the following, we shall treat the screening effect based on an RG treatment.

In an RG procedure, the contributions from the pairs with the sizes between r and $r + dr$ will be integrated out, starting from $r = a$. The probability for the vortex-antivortex pairs separated by a distance r is controlled by the pair fugacity $y^2(r)$. In the KT theory [38, 39], the initial is $y^2(a) = e^{-\beta E_c}$, (where $\beta = \frac{1}{k_B T}$ and E_c is the core energy). The renormalization effect is then represented by two renormalized quantities, $X(r) \equiv \frac{2\pi\kappa}{\beta q^2}$ and $y^2(r)$, which satisfy the following famous recursion relations

$$dy/dl = (2 - \frac{\pi}{X})\,y, \tag{81}$$

$$dX/dl = 4\pi^3 y^2, \tag{82}$$

where $r = ae^l$. From Eqs.(81)-(82), we find

$$y^2 = y_0^2 + \frac{1}{\pi^3}(X - X_0) - \frac{1}{2\pi^2}\ln\frac{X}{X_0}, \tag{83}$$

where $X_0 \equiv X(l=0) = \frac{2\pi}{\beta q^2}$ (with $\kappa(l=0)=1$). The RG flow is then obtained from Eq.(82) by

$$l = \int_{X_0}^{X} \frac{dX'}{4\pi^3 Y_0^2 + 4(X' - X_0) - 2\pi\ln(X'/X_0)}. \tag{84}$$

The pair fugacity can be determined by $y^2(l) = e^{-2\int_0^l (2-\frac{\pi}{X})dl'}$.

The RG flow diagram of Eqs.(81)-(82) is as follows: the two basins of attraction are separated by the initial values which flow to $X^* \to \frac{\pi}{2}$ and $y^* \to 0$ in the limit $l \to \infty$. In terms of Eq.(84), the separatrix of the RG flows is given by

$$l = \int_{X_0}^{X} \frac{dX'}{4(X' - \frac{\pi}{2}) - 2\pi\ln(2X'/\pi)}. \tag{85}$$

Based on the RG equation of (85), one can determine the KT temperature T_{KT}. Finally we approximately have

$$X(l) \simeq X_0 \simeq X(l \to \infty) = \frac{\pi}{2} \tag{86}$$

and

$$k_B T_{\mathrm{KT}} \simeq \frac{q^2}{4} = \frac{\pi\rho_s(0)}{2}. \tag{87}$$

For the case of $U = 15t$, $t' = 0.05t$, $\mu_1 = \mu_2 = -h = -7t$, we found a fairly low KT transition temperature as

$$k_B T_{\mathrm{KT}} = \frac{\pi\rho_s(0)}{2} \simeq 0.0045t. \tag{88}$$

Below $T_{\mathrm{KT}} \simeq 0.0045t/k_B$, we have a TSF with long range phase coherence. In the temperature region $T_{\mathrm{KT}} < T < T_c \simeq 2.25t/k_B$, we have the SF pairing but no phase coherence. And in this region, the vortex are deconfined from the bound state. At higher temperature, $T > T_c \simeq 2.25t/k_B$, the SF pairing order disappears.

VIII. CONCLUSION

In the end, we conclude our discussions. We propose a scenario in which a topological phase, possessing gapless edge states and non-Abelian anyons, is realized by proximity effect between a $\mathcal{C} = \pm 1$ topological insulator and an *s*-wave SF of ultracold fermionic atoms in a bilayer optical lattice with an effective gauge field and a layer-dependent Zeeman field generated by laser-field. At the beginning, we give an effective design of the bilayer Haldane model. Then we put two-component (two pseudo-spins) interacting fermions on this bilayer optical lattice with fixed particle concentration. For layer-1, the Haldane model of two-component fermions at 1/4 filling under a strong Zeeman field becomes a $\mathcal{C} = \pm 1$ topological insulator. While for layer-2, there is no Zeeman fields, we get an s-wave SF state by tuning the interaction between fermion via Feshbach resonance technique. Thus due to the proximity effect, we get an effective $\mathcal{C} = \pm 1$ TSF state. We also study its topological properties and then show the gapless Majorana edge modes and the non-Abelian statistics of the π-flux. This $\mathcal{C} = \pm 1$ TSF therefore may be a possible candidate for topological quantum computation. Finally we calculate the phase stiffness by using the RPA approach and then derive the temperature of the KT transition for the system.

Acknowledgments

The authors thank W. Yi and Z. W. Zhou for their helpful discussion. This work is supported by NFSC Grant No. 11174035, National Basic Research Program of China (973 Program) under the grant No. 2011CB921803, 2012CB921704.

Appendix A: Parameters in Green functions

In the appendix, we first give the elements in $Q(\mathbf{q}, \mathbf{k})$:

$$\begin{aligned} Q_{11} &= \frac{1}{\beta}\sum_{\omega_m} G_{011}(k)G_{022}(k-q) \\ Q_{12} &= \frac{1}{\beta}\sum_{\omega_m} G_{012}(k)G_{012}(k-q) \\ Q_{13} &= \frac{1}{\beta}\sum_{\omega_m} G_{014}(k)G_{032}(k-q) \\ Q_{14} &= \frac{1}{\beta}\sum_{\omega_m} G_{013}(k)G_{042}(k-q) \end{aligned} \tag{A1}$$

$$\begin{aligned} Q_{21} &= \frac{1}{\beta}\sum_{\omega_m} G_{021}(k)G_{021}(k-q) \\ Q_{22} &= \frac{1}{\beta}\sum_{\omega_m} G_{022}(k)G_{011}(k-q) \\ Q_{23} &= \frac{1}{\beta}\sum_{\omega_m} G_{024}(k)G_{031}(k-q) \\ Q_{24} &= \frac{1}{\beta}\sum_{\omega_m} G_{023}(k)G_{041}(k-q) \end{aligned} \tag{A2}$$

$$\begin{aligned}
Q_{31} &= \frac{1}{\beta}\sum_{\omega_m} G_{041}(k)G_{023}(k-q) \\
Q_{32} &= \frac{1}{\beta}\sum_{\omega_m} G_{042}(k)G_{013}(k-q) \\
Q_{33} &= \frac{1}{\beta}\sum_{\omega_m} G_{044}(k)G_{033}(k-q) \\
Q_{34} &= \frac{1}{\beta}\sum_{\omega_m} G_{043}(k)G_{043}(k-q)
\end{aligned} \tag{A3}$$

$$\begin{aligned}
Q_{41} &= \frac{1}{\beta}\sum_{\omega_m} G_{031}(k)G_{024}(k-q) \\
Q_{42} &= \frac{1}{\beta}\sum_{\omega_m} G_{032}(k)G_{014}(k-q) \\
Q_{43} &= \frac{1}{\beta}\sum_{\omega_m} G_{034}(k)G_{034}(k-q) \\
Q_{44} &= \frac{1}{\beta}\sum_{\omega_m} G_{033}(k)G_{044}(k-q).
\end{aligned} \tag{A4}$$

Here we have

$$G_{0ij}(\mathbf{k}) = \frac{A_{ij}}{\mathrm{i}\omega_m - e_{1,\mathbf{k}}} + \frac{B_{ij}}{\mathrm{i}\omega_m + e_{1,\mathbf{k}}} + \frac{C_{ij}}{\mathrm{i}\omega_m - e_{2,\mathbf{k}}} + \frac{D_{ij}}{\mathrm{i}\omega_m + e_{2,\mathbf{k}}}, \tag{A5}$$

where the parameters A_{ij}, B_{ij}, C_{ij}, D_{ij} in $G_{0ij}(\mathbf{k})$ are given by

$$\begin{aligned}
A_{11}(\mathbf{k}) &= \frac{1+p_{11}(\mathbf{k})}{4} - \frac{\gamma_{\mathbf{k}} - \mu + q_{11}(\mathbf{k})}{4e_1} \\
B_{11}(\mathbf{k}) &= \frac{1+p_{11}(\mathbf{k})}{4} + \frac{\gamma_{\mathbf{k}} - \mu + q_{11}(\mathbf{k})}{4e_1} \\
C_{11}(\mathbf{k}) &= \frac{1-p_{11}(\mathbf{k})}{4} - \frac{\gamma_{\mathbf{k}} - \mu - q_{11}(\mathbf{k})}{4e_1} \\
D_{11}(\mathbf{k}) &= \frac{1-p_{11}(\mathbf{k})}{4} + \frac{\gamma_{\mathbf{k}} - \mu + q_{11}(\mathbf{k})}{4e_1}
\end{aligned} \tag{A6}$$

with

$$\begin{aligned}
p_{11}(\mathbf{k}) &= \frac{-\mu\gamma_{\mathbf{k}}}{\sqrt{\gamma_{\mathbf{k}}^2[\mu^2+\Delta_0^2\,]+|\xi_{\mathbf{k}}|^2\mu^2}} \\
q_{11}(\mathbf{k}) &= \frac{\gamma_{\mathbf{k}}(\mu^2+\Delta_0^2\,) - \mu(\gamma_{\mathbf{k}}^2+|\xi_{\mathbf{k}}|^2)}{\sqrt{\gamma_{\mathbf{k}}^2[\mu^2+\Delta_0^2\,]+|\xi_{\mathbf{k}}|^2\mu^2}}
\end{aligned} \tag{A7}$$

and

$$\begin{aligned}
A_{12}(\mathbf{k}) &= \frac{p_{12}(\mathbf{k})}{4} + \frac{\Delta_0\; - q_{12}(\mathbf{k})}{4e_1} \\
B_{12}(\mathbf{k}) &= \frac{p_{12}(\mathbf{k})}{4} - \frac{\Delta_0\; - q_{12}(\mathbf{k})}{4e_1} \\
C_{12}(\mathbf{k}) &= \frac{-p_{12}(\mathbf{k})}{4} + \frac{\Delta_0 + q_{12}(\mathbf{k})}{4e_2} \\
D_{12}(\mathbf{k}) &= \frac{-p_{12}(\mathbf{k})}{4} - \frac{\Delta_0 + q_{12}(\mathbf{k})}{4e_2}
\end{aligned} \tag{A8}$$

with

$$\begin{aligned}
p_{12}(\mathbf{k}) &= \frac{-\gamma_{\mathbf{k}}\Delta_0}{\sqrt{\gamma_{\mathbf{k}}^2[\mu^2+\Delta_0^2\,]+|\xi_{\mathbf{k}}|^2\mu^2}} \\
q_{12}(\mathbf{k}) &= \frac{-\Delta_0\;\gamma_k^2}{\sqrt{\gamma_{\mathbf{k}}^2[\mu^2+\Delta_0^2\,]+|\xi_{\mathbf{k}}|^2\mu^2}}
\end{aligned} \tag{A9}$$

and

$$\begin{aligned}
A_{13}(\mathbf{k}) &= \frac{p_{13}(\mathbf{k})}{4} - \frac{\xi_{\mathbf{k}} + q_{13}(\mathbf{k})}{4e_1} \\
B_{13}(\mathbf{k}) &= \frac{p_{13}(\mathbf{k})}{4} + \frac{\xi_{\mathbf{k}} + q_{13}(\mathbf{k})}{4e_1} \\
C_{13}(\mathbf{k}) &= \frac{-p_{13}(\mathbf{k})}{4} - \frac{\xi_{\mathbf{k}} - q_{13}(\mathbf{k})}{4e_2} \\
D_{13}(\mathbf{k}) &= \frac{-p_{13}(\mathbf{k})}{4} + \frac{\xi_{\mathbf{k}} - q_{13}(\mathbf{k})}{4e_2}
\end{aligned} \tag{A10}$$

with

$$\begin{aligned}
p_{13}(\mathbf{k}) &= \frac{-\mu\xi_{\mathbf{k}}}{\sqrt{\gamma_{\mathbf{k}}^2[\mu^2+\Delta_0^2\,]+|\xi_{\mathbf{k}}|^2\mu^2}} \\
q_{13}(\mathbf{k}) &= \frac{\xi_{\mathbf{k}}\mu^2}{\sqrt{\gamma_{\mathbf{k}}^2[\mu^2+\Delta_0^2\,]+|\xi_{\mathbf{k}}|^2\mu^2}}
\end{aligned} \tag{A11}$$

and

$$\begin{aligned}
A_{14}(\mathbf{k}) &= \frac{-q_{14}(\mathbf{k})}{4e_1} \\
B_{14}(\mathbf{k}) &= \frac{q_{14}(\mathbf{k})}{4e_1} \\
C_{14}(\mathbf{k}) &= \frac{q_{14}(\mathbf{k})}{4e_2} \\
D_{14}(\mathbf{k}) &= \frac{-q_{14}(\mathbf{k})}{4e_2}
\end{aligned} \tag{A12}$$

with

$$q_{14}(\mathbf{k}) = \frac{\xi_{\mathbf{k}}\Delta_0\;(\gamma_{\mathbf{k}}+\mu)}{\sqrt{\gamma_{\mathbf{k}}^2[\mu^2+\Delta_0^2\,]+|\xi_{\mathbf{k}}|^2\mu^2}} \tag{A13}$$

and

$$\begin{aligned}
A_{21}(\mathbf{k}) &= A_{12}^*(\mathbf{k}) \\
B_{21}(\mathbf{k}) &= B_{12}^*(\mathbf{k}) \\
C_{21}(\mathbf{k}) &= C_{12}^*(\mathbf{k}) \\
D_{21}(\mathbf{k}) &= D_{12}^*(\mathbf{k})
\end{aligned} \tag{A14}$$

and

$$\begin{aligned}
A_{22}(\mathbf{k}) &= \frac{1+p_{22}(\mathbf{k})}{4} - \frac{\gamma_{\mathbf{k}} + \mu + q_{22}(\mathbf{k})}{4e_1} \\
B_{22}(\mathbf{k}) &= \frac{1+p_{22}(\mathbf{k})}{4} + \frac{\gamma_{\mathbf{k}} + \mu + q_{22}(\mathbf{k})}{4e_1} \\
C_{22}(\mathbf{k}) &= \frac{1-p_{22}(\mathbf{k})}{4} - \frac{\gamma_{\mathbf{k}} + \mu - q_{22}(\mathbf{k})}{4e_2} \\
D_{22}(\mathbf{k}) &= \frac{1-p_{22}(\mathbf{k})}{4} + \frac{\gamma_{\mathbf{k}} + \mu - q_{22}(\mathbf{k})}{4e_2}
\end{aligned} \tag{A15}$$

with

$$\begin{aligned}p_{22}(\mathbf{k}) &= \frac{\mu\gamma_{\mathbf{k}}}{\sqrt{\gamma_{\mathbf{k}}^2[\mu^2+\Delta_0^2\,]+|\xi_{\mathbf{k}}|^2\mu^2}}\\ q_{22}(\mathbf{k}) &= \frac{\gamma_{\mathbf{k}}(\mu^2+\Delta_0^2\,)+\mu(\gamma_k^2+|\xi_{\mathbf{k}}|^2)}{\sqrt{\gamma_{\mathbf{k}}^2[\mu^2+\Delta_0^2\,]+|\xi_{\mathbf{k}}|^2\mu^2}}\end{aligned}\tag{A16}$$

and

$$\begin{aligned}A_{23}(\mathbf{k}) &= \frac{-q_{23}(\mathbf{k})}{4e_1}\\ B_{23}(\mathbf{k}) &= \frac{q_{23}(\mathbf{k})}{4e_1}\\ C_{23}(\mathbf{k}) &= \frac{q_{23}(\mathbf{k})}{4e_2}\\ D_{23}(\mathbf{k}) &= \frac{-q_{23}(\mathbf{k})}{4e_2}\end{aligned}\tag{A17}$$

with

$$q_{23}(\mathbf{k}) = \frac{-\xi\Delta_0\,(\gamma_{\mathbf{k}}-\mu)}{\sqrt{\gamma_{\mathbf{k}}^2[\mu^2+\Delta_0^2\,]+|\xi_{\mathbf{k}}|^2\mu^2}}\tag{A18}$$

and

$$\begin{aligned}A_{24}(\mathbf{k}) &= \frac{p_{24}(\mathbf{k})}{4}+\frac{\xi_{\mathbf{k}}-q_{24}(\mathbf{k})}{4e_1}\\ B_{24}(\mathbf{k}) &= \frac{p_{24}(\mathbf{k})}{4}-\frac{\xi_{\mathbf{k}}-q_{24}(\mathbf{k})}{4e_1}\\ C_{24}(\mathbf{k}) &= \frac{-p_{24}(\mathbf{k})}{4}+\frac{\xi_{\mathbf{k}}+q_{24}(\mathbf{k})}{4e_2}\\ D_{24}(\mathbf{k}) &= \frac{-p_{24}(\mathbf{k})}{4}-\frac{\xi_{\mathbf{k}}+q_{24}(\mathbf{k})}{4e_2}\end{aligned}\tag{A19}$$

with

$$\begin{aligned}p_{24}(\mathbf{k}) &= \frac{-\mu\xi_{\mathbf{k}}}{\sqrt{\gamma_{\mathbf{k}}^2[\mu^2+\Delta_0^2\,]+|\xi_{\mathbf{k}}|^2\mu^2}}\\ q_{24}(\mathbf{k}) &= \frac{-\xi_{\mathbf{k}}\mu^2}{\sqrt{\gamma_{\mathbf{k}}^2[\mu^2+\Delta_0^2\,]+|\xi_{\mathbf{k}}|^2\mu^2}}\end{aligned}\tag{A20}$$

and

$$\begin{aligned}A_{31}(\mathbf{k}) &= A_{13}^*(\mathbf{k})\\ B_{31}(\mathbf{k}) &= B_{13}^*(\mathbf{k})\\ C_{31}(\mathbf{k}) &= C_{13}^*(\mathbf{k})\\ D_{31}(\mathbf{k}) &= D_{13}^*(\mathbf{k})\end{aligned}\tag{A21}$$

and

$$\begin{aligned}A_{32}(\mathbf{k}) &= A_{23}^*(\mathbf{k})\\ B_{32}(\mathbf{k}) &= B_{23}^*(\mathbf{k})\\ C_{32}(\mathbf{k}) &= C_{23}^*(\mathbf{k})\\ D_{32}(\mathbf{k}) &= D_{23}^*(\mathbf{k})\end{aligned}\tag{A22}$$

and

$$\begin{aligned}A_{33}(\mathbf{k}) &= \frac{1+p_{33}(\mathbf{k})}{4}+\frac{\gamma_{\mathbf{k}}+\mu-q_{33}(\mathbf{k})}{4e_1}\\ B_{33}(\mathbf{k}) &= \frac{1+p_{33}(\mathbf{k})}{4}-\frac{\gamma_{\mathbf{k}}+\mu-q_{33}(\mathbf{k})}{4e_1}\\ C_{33}(\mathbf{k}) &= \frac{1-p_{33}(\mathbf{k})}{4}+\frac{\gamma_{\mathbf{k}}+\mu+q_{33}(\mathbf{k})}{4e_2}\\ D_{33}(\mathbf{k}) &= \frac{1-p_{33}(\mathbf{k})}{4}-\frac{\gamma_{\mathbf{k}}+\mu+q_{33}(\mathbf{k})}{4e_2}\end{aligned}\tag{A23}$$

with

$$\begin{aligned}p_{33}(\mathbf{k}) &= \frac{\mu\gamma_{\mathbf{k}}}{\sqrt{\gamma_{\mathbf{k}}^2[\mu^2+\Delta_0^2\,]+|\xi_{\mathbf{k}}|^2\mu^2}}\\ q_{33}(\mathbf{k}) &= \frac{-\gamma_{\mathbf{k}}(\mu^2+\Delta_0^2\,)-\mu(\gamma_{\mathbf{k}}^2+|\xi_{\mathbf{k}}|^2)}{\sqrt{\gamma_{\mathbf{k}}^2[\mu^2+\Delta_0^2\,]+|\xi_{\mathbf{k}}|^2\mu^2}}\end{aligned}\tag{A24}$$

and

$$\begin{aligned}A_{34}(\mathbf{k}) &= \frac{p_{34}(\mathbf{k})}{4}+\frac{\Delta_0\ -q_{34}(\mathbf{k})}{4e_1}\\ B_{34}(\mathbf{k}) &= \frac{p_{34}(\mathbf{k})}{4}-\frac{\Delta_0\ -q_{34}(\mathbf{k})}{4e_1}\\ C_{34}(\mathbf{k}) &= \frac{-p_{34}(\mathbf{k})}{4}+\frac{\Delta_0\ +q_{34}(\mathbf{k})}{4e_2}\\ D_{34}(\mathbf{k}) &= \frac{-p_{34}(\mathbf{k})}{4}-\frac{\Delta_0\ +q_{34}(\mathbf{k})}{4e_2}\end{aligned}\tag{A25}$$

with

$$\begin{aligned}p_{34}(\mathbf{k}) &= \frac{\Delta_0\ \gamma_{\mathbf{k}}}{\sqrt{\gamma_{\mathbf{k}}^2[\mu^2+\Delta_0^2\,]+|\xi_{\mathbf{k}}|^2\mu^2}}\\ q_{34}(\mathbf{k}) &= \frac{-\Delta_0\ \gamma_{\mathbf{k}}^2}{\sqrt{\gamma_{\mathbf{k}}^2[\mu^2+\Delta_0^2\,]+|\xi_{\mathbf{k}}|^2\mu^2}}\end{aligned}\tag{A26}$$

and

$$\begin{aligned}A_{41}(\mathbf{k}) &= A_{14}^*(\mathbf{k})\\ B_{41}(\mathbf{k}) &= B_{14}^*(\mathbf{k})\\ C_{41}(\mathbf{k}) &= C_{14}^*(\mathbf{k})\\ D_{41}(\mathbf{k}) &= D_{14}^*(\mathbf{k})\end{aligned}\tag{A27}$$

and

$$\begin{aligned}A_{42}(\mathbf{k}) &= A_{24}^*(\mathbf{k})\\ B_{42}(\mathbf{k}) &= B_{24}^*(\mathbf{k})\\ C_{42}(\mathbf{k}) &= C_{24}^*(\mathbf{k})\\ D_{42}(\mathbf{k}) &= D_{24}^*(\mathbf{k})\end{aligned}\tag{A28}$$

and

$$\begin{aligned}A_{43}(\mathbf{k}) &= A_{34}^*(\mathbf{k})\\ B_{43}(\mathbf{k}) &= B_{34}^*(\mathbf{k})\\ C_{43}(\mathbf{k}) &= C_{34}^*(\mathbf{k})\\ D_{43}(\mathbf{k}) &= D_{34}^*(\mathbf{k})\end{aligned}\tag{A29}$$

and

$$\begin{aligned}
A_{44}(\mathbf{k}) &= \frac{1+p_{44}(\mathbf{k})}{4} - \frac{-\gamma_{\mathbf{k}}+\mu+q_{44}(\mathbf{k})}{4e_1} \\
B_{44}(\mathbf{k}) &= \frac{1+p_{44}(\mathbf{k})}{4} + \frac{-\gamma_{\mathbf{k}}+\mu+q_{44}(\mathbf{k})}{4e_1} \\
C_{44}(\mathbf{k}) &= \frac{1-p_{44}(\mathbf{k})}{4} - \frac{-\gamma_{\mathbf{k}}+\mu-q_{44}(\mathbf{k})}{4e_2} \\
D_{44}(\mathbf{k}) &= \frac{1-p_{44}(\mathbf{k})}{4} + \frac{-\gamma_{\mathbf{k}}+\mu-q_{44}(\mathbf{k})}{4e_2}
\end{aligned} \tag{A30}$$

with

$$\begin{aligned}
p_{44}(\mathbf{k}) &= \frac{-\mu\gamma_{\mathbf{k}}}{\sqrt{\gamma_{\mathbf{k}}^2[\mu^2+\Delta_0^2\,]+|\xi_{\mathbf{k}}|^2\mu^2}} \\
q_{44}(\mathbf{k}) &= \frac{-\gamma_{\mathbf{k}}(\mu^2+\Delta_0^2\,)+\mu(\gamma_{\mathbf{k}}^2+|\xi_{\mathbf{k}}|^2)}{\sqrt{\gamma_{\mathbf{k}}^2[\mu^2+\Delta_0^2\,]+|\xi_{\mathbf{k}}|^2\mu^2}}.
\end{aligned} \tag{A31}$$

The detailed forms of elements in matrix M are given as follows:

$$\begin{aligned}
W_{11} &= \frac{1}{2N}\sum_{\mathbf{k}}(Q_{11}+Q_{21}+Q_{12}+Q_{22}) \\
W_{12} &= \frac{1}{2N}\sum_{\mathbf{k}} i(Q_{11}+Q_{21})-i(Q_{12}+Q_{22}) \\
W_{13} &= \frac{1}{2N}\sum_{\mathbf{k}} -i(Q_{13}+Q_{23})+i(Q_{14}+Q_{24}) \\
W_{14} &= \frac{1}{2N}\sum_{\mathbf{k}}(Q_{13}+Q_{23}+Q_{14}+Q_{24})
\end{aligned} \tag{A32}$$

$$\begin{aligned}
W_{21} &= \frac{1}{2N}\sum_{\mathbf{k}} -i(Q_{11}-Q_{21})-i(Q_{12}-Q_{22}) \\
W_{22} &= \frac{1}{2N}\sum_{\mathbf{k}}(Q_{11}-Q_{21}-Q_{12}+Q_{22}) \\
W_{23} &= \frac{1}{2N}\sum_{\mathbf{k}}(-Q_{13}+Q_{23}+Q_{14}-Q_{24}) \\
W_{24} &= \frac{1}{2N}\sum_{\mathbf{k}} -i(Q_{13}-Q_{23})-i(Q_{14}-Q_{24})
\end{aligned} \tag{A33}$$

$$\begin{aligned}
W_{31} &= \frac{1}{2N}\sum_{\mathbf{k}} i(Q_{31}-Q_{41})+i(Q_{32}-Q_{42}) \\
W_{32} &= \frac{1}{2N}\sum_{\mathbf{k}}(-Q_{31}+Q_{32}+Q_{41}-Q_{42}) \\
W_{33} &= \frac{1}{2N}\sum_{\mathbf{k}}(Q_{33}-Q_{43}-Q_{34}-Q_{44}) \\
W_{34} &= \frac{1}{2N}\sum_{\mathbf{k}} i(Q_{33}-Q_{43})+i(Q_{34}-Q_{44})
\end{aligned} \tag{A34}$$

$$\begin{aligned}
W_{41} &= \frac{1}{2N}\sum_{\mathbf{k}}(Q_{31}+Q_{41}+Q_{32}+Q_{42}) \\
W_{42} &= \frac{1}{2N}\sum_{\mathbf{k}} i(Q_{31}+Q_{41})-i(Q_{32}+Q_{42}) \\
W_{43} &= \frac{1}{2N}\sum_{\mathbf{k}} -i(Q_{33}+Q_{43})+i(Q_{34}+Q_{44}) \\
W_{44} &= \frac{1}{2N}\sum_{\mathbf{k}}(Q_{33}+Q_{43}+Q_{34}+Q_{44}).
\end{aligned} \tag{A35}$$

[1] A. Kitaev, Ann. Phys. **321**, 2-111 (2006).

[2] M. Freedman, M. Larsen, and Z. Wang, Commun. Math. Phys. **227**, 605-622 (2002).

[3] J. Eisenstein, K. Cooper, L. Pfeiffer, and K. West, Phys. Rev. Lett. **88**, 076801 (2002).

[4] J. Xia, W. Pan, C. L. Vicente, E. D. Adams, N. S. Sullivan, H. L. Stormer, D. C. Tsui, L. N. Pfeiffer, K. W. Baldwin, and K. W. West, Phys. Rev. Lett. **93**, 176809 (2004).

[5] S. Das Sarma, C. Nayak, and S. Tewari, Phys. Rev. B **73**, 220502 (2006).

[6] J. Alice, Y. Oreg, G. Refael, F. von Oppen, and M. P. A. Fisher, Nature Physics **7**, 412 (2011).

[7] L. Fu, and C. L. Kane, Phys. Rev. Lett. **100**, 096407 (2008).

[8] M. Greiner, O. Mandel, T. Esslinger, T. W. Hänsch, and I. Bloch, Nature **415**, 39-44 (2002).

[9] D. Jaksch, C. Bruder, J. I. Cirac, C. W. Gardiner, and P. Zoller, Phys. Rev. Lett. **81**, 3108 (1998).

[10] M. Lewenstein, A. Sanpera, V. Ahufinge, B. Damski, A. Sen(De), and U. Sen, Advances in Physics **56**, 243-379 (2007).

[11] I. Bloch, J. Dalibard, and W. Zwerger, Rev. Mod. Phys. **80**, 885 (2008).

[12] G. Juzeliunas, and P. Ohberg, *Optical Manipulation of Ultracold Atoms, In: Structured Light and its Applica-*

tions (Elevier, Amsterdam, 2008).

[13] L. B. Shao, Shi-Liang Zhu, Li. Sheng, D. Y. Xing, and Z. D. Wang, Phys. Rev. Lett. **101**, 246810 (2008).

[14] I. B. Spielman, Phys. Rev. A **79**, 063613 (2009).

[15] Y.-J. Lin, R. L. Compton, A. R. Perry, W. D. Phillips, J. V. Porto, and I. B. Spielman, Phys. Rev. Lett. **102**, 130401 (2009).

[16] Y.-J. Lin, R. L. Compton, K. Jiménez-García, J. V. Porto, and I. B. Spielman, Nature **462**, 628-632 (2009).

[17] Y.-J. Lin, R. L. Compton, K. Jiménez-García, and I. B. Spielman, Nature **471**, 83-86 (2011).

[18] M. Aidelsburger, M. Atala, S. Nascimbène, S. Trotzky, Y.-A. Chen, and I. Bloch, Phys. Rev. Lett. **107**, 255301 (2011).

[19] S. L. Zhu, B. Wang, L.-M. Duan, Phys. Rev. Lett. **98**, 260402 (2007).

[20] S. Coleman, Phys. Rev. D **15**, 2929 (1977).

[21] C. G. Callan Jr. and S. Coleman, Phys. Rev. D **16**, 1762 (1977).

[22] K. L. Lee, B. Gréaud, R. Han, B.-G. Englert, and C. Miniatura, Phys. Rev. A **80**, 043411 (2009).

[23] F. D. M. Haldane, Phys. Rev. Lett. **61**, 2015 (1988).

[24] T. Köhler and K. Góral, and Paul S. Julienne, Rev. Mod. Phys. **78**, 1311-1361 (2006).

[25] C. Chin, R. Grimm, P. Julienne, and E. Tiesinga, Rev. Mod. Phys. **82**, 1225-1286 (2010).

[26] S. A. Morgan, M. D. Lee, and K. Burnett, Phys. Rev. A **65**, 022706 (2002).

[27] J. He, S. P. Kou, Y. Liang, and S. P. Feng, Phys. Rev. B **83**, 205116 (2011).

[28] J. He, Y. H Zong, S. P. Kou, Y. Liang, and S. P. Feng, Phys. Rev. B **84**, 035127 (2011).

[29] D. J. Thouless, M. Kohmoto, M. P. Nightingale, and M. den Nijs, Phys. Rev. Lett. **49**, 405 (1982).

[30] X. L. Qi, Taylor L. Hughes, and S. C. Zhang, Phys. Rev. B **82**, 184516 (2010).

[31] X. Liu, Z. Wang, X. C. Xie, & Y. Yu, Phys. Rev. B **83**, 125105 (2011).

[32] N. Read, and D. Green, Phys. Rev. B **61**, 10267-10297 (2000).

[33] D. A. Ivanov, Phys. Rev. Lett. **86**, 268 (2001).

[34] G. Moore, and N. Read, Nucl. Phys. B **360**, 362-396 (1991).

[35] M. Iskin and C. A. R. Sá de Melo, Phys. Rev. B **72**, 024512 (2005).

[36] E. Taylor, A. Griffin, N. Fukushima and Y. Ohashi, Phys. Rev. A **74**, 063626 (2006).

[37] E. Zhao and A. Paramekanti, Phys. Rev. Lett. **97**, 230404 (2006).

[38] V. L Berezinskii, Sov. Phys. JETP **34**, 610 (1972).

[39] J. M. Kosterlitz, and D. J. Thouless, J. Phys. C **6**, 1181-1203 (1973).